Electronic supplementary information (ESI)

Optomagnetic detection of DNA nanoswitches

Gabriel Antonio S. Minero,[a,b] Jeppe Fock,[a] John S. McCaskill,[b] and Mikkel F. Hansen[a]

[a]Department of Micro- and Nanotechnology, Technical University of Denmark, DTU Nanotech, Building 345B, DK-2800 Kongens Lyngby, Denmark.

[b]Ruhr-Universitaet Bochum, Microsystems Chemistry and BioIT (BioMIP), NC3, Universitaetsstr. 150, 44801 Bochum, GERMANY.

S1: Optomagnetic method and setup

The transmission of monochromatic light ($\lambda = 405$ nm) through a suspension of MNPs or agglomerates of MNPs is detected using a photodetector. Coils positioned on both sides of the suspension produce a sinusoidally varying homogeneous magnetic field in the direction of the light path. The oscillating magnetic field forces the MNPs to cyclically align towards and relax away from the magnetic field direction resulting in a modulation of the intensity of transmitted light. The transmission depends only on the magnitude and not on the direction of the magnetic field. This results in the signal being detected in the second harmonic response, V_2, of the applied field frequency. The spectra of the complex 2nd harmonic signal ($V_2 = V_2' + \mathrm{i}V_2''$) are normalised with the average intensity of transmitted light (V_0).

The optomagnetic method relies on the coupled magnetic and optical anisotropies of the MNPs or agglomerates of MNPs. Particles aligned with the magnetic field giving rise to a higher intensity of transmitted light will result in a negative sign of V_2. Depending on the size-dependence of the extinction properties of the MNPs (and clusters of MNPs), the signal can also decrease when they align with the field resulting in a positive sign of V_2.

To obtain the relaxation properties of the MNPs, V_2 is measured as a function of frequency f of the applied magnetic field. The hydrodynamic volume of the MNP is inversely proportional to the zero crossing observed in V_2'', which corresponds to the (rotational) Brownian relaxation frequency:

$$f_{\mathrm{B}} = \frac{k_{\mathrm{B}}T}{\pi^2 \eta D_{\mathrm{h}}^3}, \tag{1}$$

where f_{B} is Boltzmann's constant, T is the absolute temperature, η is the dynamic viscosity of the liquid and D_h is the hydrodynamic diameter of the MNPs. Also the peak position in V_2' is related to f_{B} although not equal to it.

The optomagnetic measurements were performed in a cuvette setup and a disc based setup both using blue lasers ($\lambda = 405$ nm). In the cuvette setup, a commercial plastic cuvette was used (Sarstedt AG & Co.) with an optical path length of 2 mm and the magnetic field amplitude was 0.5 mT. The disc-based setup had an optical path length of 0.9 mm and the field amplitude was 1.7 mT. The discs were fabricated as previously reported.[1] For magnetic incubation, the cuvette was placed in the centre of a uniform magnetic field (20 mT) for 2 min whereas the disc was sequentially shaken under a permanent magnet (220 mT) for 4 s followed by 8 s of shaking outside the magnet to remove unspecific agglomerates formed during the magnetic incubation. The measurement and motor control were automated using commercial Labview software. The on-disc shaking and magnetic incubation were performed using the sequential measurement protocol.[1] In total, 30 cycles of magnetic incubation were performed for each measurement.

All spectra were measured in 20 logarithmically equidistant steps between f = 1 and 3200 Hz. A spectrum was measured in about 1 min.

S2: Materials and Methods

DNA binding assay

Streptavidin (STV) beads (BNF-Starch, Micromod, Germany), 100 nm, were functionalised with biotinylated DNA molecules in the binding buffer for 60 min. A saturation step of the streptavidin binding sites (with DNA **A**) was necessary to avoid unspecific agglutination of the beads at intermediate and low probe densities. The beads were subsequently washed three times in the binding buffer. The binding buffer contained 8 mM tris, 4 mM EDTA, 0.1 % Tween-20, and 0.8 M NaCl. The buffer pH was adjusted by 1 M HCl and checked with pH-meter as well as a paper pH indicator.

For estimation of the number of probes per MNP, two populations of beads, 1 mg/ml, were functionalised with 20, 40, 60, and 80 nM DNA probes **P1** and **P3**. After saturation and washing steps, the functionalised beads were subsequently used for depletion of the complementary target **TF**.

Else, for assays employing triplex mediated MNP agglutination, 1 mg/ml beads were mixed with 20-150 nM of pre-annealed biotinylated duplex (ds) **A·Y.** The functionalised beads, 0.2 mg/ml, were used for aggregation in the presence of 0.05 nM -2 nM *ss* **R**. For negative controls, DNA **B** was used.

DNA **A**, **Y**, and **R** were ordered from IBA (Germany) with *HPLC purification grade*. DNA **B, P1, P3, and TF** were ordered from DNA Technologies (Denmark) with *HPLC purification grade*. All DNA sequences employed are listed in Table S1.

Table S1: DNA sequences. Tagged bases in **P1** and **P3** DNA sequences contain 2'-O-Me modifications for more stable binding of the target **TF**.

Code	DNA Sequence (5' → 3')	Comment
A	TCG AGT CTG TTG ACG	5'biotin
B	GCT TGA GTC TCG TAG AGG GGG GTT CGC CAC CGG TAT TCC T	NC
R	GGG AAG GAG AAA AAA GAG GAA GGG	t-DNA
Y	CCC TTC CTC TTT TTT CTC CTT CCC CGT CAA CAG ACT CGA	p-DNA
P1	G$\hat{A}$C T$\hat{A}$T A$\hat{C}$T G$\hat{A}$G GAG TTTTTTTTTTTTTTTTTTT	5'biotin
P3	TTTTTTTTTTTTTTTTTTT C$\hat{T}$G $\hat{C}$A$\hat{T}$ A$\hat{C}$A CTC T	5'biotin
TF	CTC CTC AGT ATA GTC AGA GTG TAT GCA G	5'TYE563

Quantification of probes per MNP

For the quantification of probe density, a test-system of probes **P1** and **P3** as well as fluorescent target **TF** was used (Table S1). We consider binding of biotinylated DNA molecules to be independent of the nucleobase sequence (Fig. S1). In a standard assay, 20 µL of functionalised beads (1 mg/ml) were incubated with 100 µl of fluorescence labelled target (20 nM) in 60 min to allow complete hybridisation. The supernatant was added to a new tube and the remaining beads were washed with 120 µl of buffer, which was subsequently added to the new tube, now containing the unbound fluorescence DNA targets. To remove any remaining MNPs in the supernatant, 200 µl (out of 220 µl) was added to a microplate using magnetic separation and the fluorescence was measured using a plate reader. The concentration, c, of each solution was deduced from a standard curve constructed from fluorescence measurements of the **TF** DNA target concentrations. Finally, the amount of unbound DNA was calculated.

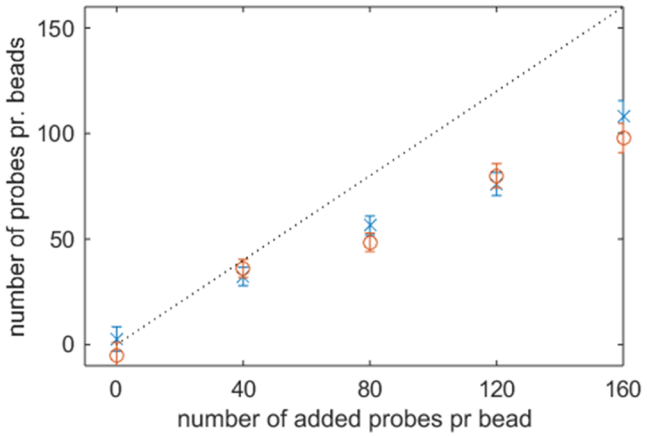

Fig. S1: Retro-quantification of DNA probe after depletion of the fluorescent target **TF** on probes **P1** and **P3**. The obtained trend is consistent with the statement (from magnetic nanoparticle provider Micromod) that 1 mg/ml MNP solution can bind *ca.* 130 nM DNA. Beads functionalised with probes **P1** revealed the same binding capacity as the ones with **P3**.

We selected for further examination an intermediate (*ca*. 50 probes per bead) as well as one of the highest (*ca*. 100 probes per bead) probe densities.

S3: Magnetic incubation

In this section, we report on accelerated solid phase triplex hybridisation after magnetic incubation. For the functionalised beads, no agglutination without magnetic incubation was observed after 5 min incubation in the presence of 1 nM target (compare (A) and (C) in Fig. S2). However, after 2 h, large aggregates were formed (Fig. S2,B). After 12 h, the large aggregates of functionalised nanoparticles sedimented and could be also observed by eye. Visual inspection of aggregates revealed correlation between their size and number of probes per nanoparticle since larger aggregates sediment faster (Fig. S2,D).

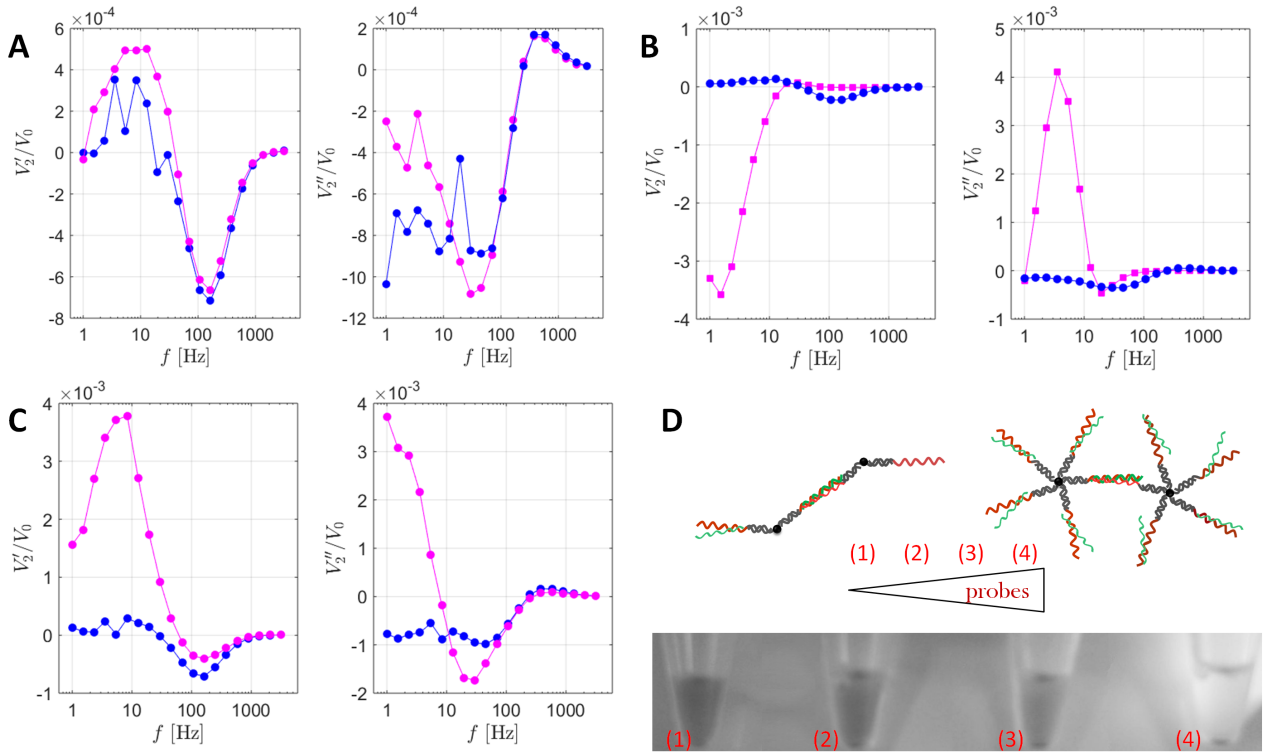

Fig. S2: optomagnetic detection of nanoparticle clusters mediated by DNA triplex formation. Data are shown as spectra of the in-phase (V_2'/V_0) and out-of-phase (V_2''/V_0) 2nd harmonic of transmitted light signal V_2 normalised with average intensity of transmitted light, V_0. Spectra obtained after (A) 5 min and (B) 2 hours of incubation with no applied magnetic field for pH 7.5 (blue) and 5.5 (pink). Virtually no signal difference is observed after 5 min (no clustering) and a large effect is observed at low frequencies after 2 h (strong clustering at pH 5.5). (C) Spectra obtained after 5 min of incubation with applied magnetic field (1 min). (D) Observation of sedimentation (depending on the p-DNA density), after 12 h, no magnetic incubation. Beads 0.2 mg/ml, probes/MNP: (**1**) 25, (**2**) 50, (**3**) 75, and (**4**) 100 (see Fig. S1).

S4: Depletion of MNP clusters through triplex DNA melting

As additional supporting information, we compare isothermal pH cycles of bead clusters and depletion of the clusters through DNA melting at conditions favouring triplex DNA formation, pH 5-6, (Fig. S3,A). We measured optomagnetic spectra between 8 and 1024 Hz in order to shorten data acquisition time in the melting experiments (this is a disadvantage of measuring at 1-10 Hz, since this range of frequencies needs longer acquisition time). We demonstrate that we can switch clusters of nanoparticles through altering conformation of the triplex DNA linking nanoparticles. While this DNA conformation can be melted at *ca*. 50 °C, we demonstrate reversible switching of the functionalised nanomaterial can be achieved at room temperature via pH cycling (Fig. S3,B).

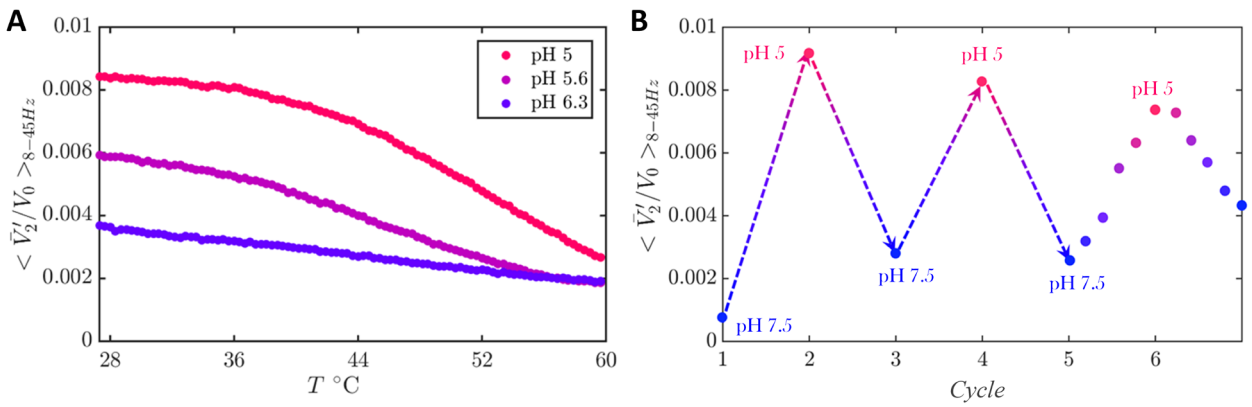

Fig. S3: thermal vs. isothermal switching of clusters assembled via triplex DNA. (A) Melting of triplex DNA followed by loss of nano-particle clusters at increasing temperature (0.5°/min) in optomagnetic signal (here, $\langle V_2'/V_0 \rangle_{8-45\,\mathrm{Hz}}$). (B) Cycling DNA conformations between conditions favouring and inhibiting triplex formation.

S5: Target dose-response analysis

We demonstrate that we can detect 0.1-2 nM polypurine target (Fig. 2) via triplex DNA folding at pH 5. Discussion of the optomagnetic spectra in the main manuscript led to the conclusion that the most obvious dose-dependent change in the signal with respect to the target concentration can be observed in V_2''/V_0.

Optomagnetic spectra

In Fig. S4, we exemplify optomagnetic spectra of the target-free functionalised MNPs (open circles) as well as in the presence of 1 nM target DNA at two critical pH values. The second harmonic spectra are composed from real, V_2'/V_0, and imaginary parts, V_2''/V_0. As discussed, triplex-mediated aggregates of the MNPs can be observed in a positive peak at low frequencies in V_2'/V_0 (8-45 Hz) as well as V_2''/V_0 (1-10 Hz). At the same time, depletion of single MNPs was observed in V_2'/V_0 (*ca.* 200 Hz) solely in response to addition of the matching target to the system at pH 5 (Fig. S4,A). However, at a certain size of aggregates, the V_2'/V_0 spectra change sign at frequencies below 10 Hz as illustrated for 2 h incubation of the functionalised MNPs in the presence of the target (Fig. S2,B). Both effects (depletion of MNPs and aggregation) lead to increase of the optomagnetic signal V_2''/V_0 at lower frequencies (Fig S4,D). Dose-dependent aggregation can be followed in both V_2'/V_0 (Fig. S4,A-C) and V_2''/V_0 (Fig. S4,D-F), however the target-mediated clustering is better distinguished from negative controls and high pH measurements by the sign of the $< V_2''/V_0 >_{1-10Hz}$ (Fig. S4,D-F).

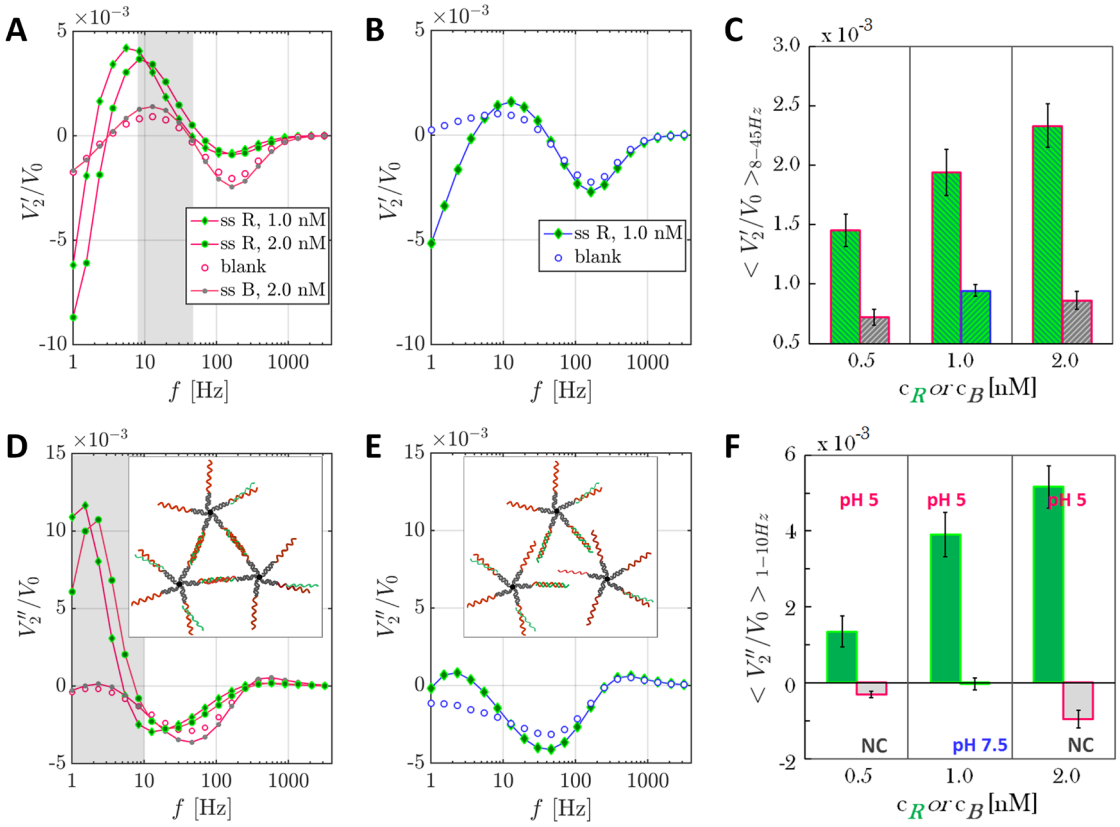

Fig. S4: optomagnetic spectra of triplex-mediated MNP aggregates under conditions favoring (A,D) and inhibiting (B,E) the triplex formation, pH 5 and 7.5, respectively. Comparison of the optomagnetic signal obtained for the matching (green) and non-matching (grey) DNA at pH 5. (C,F) Histograms summarising detection outputs of sequence-specific vs. unspecific clustering of MNPs.

Probe density

Further, we compare the dose-response analysis of the two probe densities of the functionalised MNPs, 100 and 50 probes per nanoparticle (Fig. S5). These densities correspond to *ca*. 10 nM and 5 nM of the probes, respectively, in suspension of the functionalised MNP of concentration 0.2 mg/ml. For the dense layer of probes, we obtained higher limit of detection than for the intermediate probe density, i.e. 0.5 nM instead of 0.2 nM. Taking into account optimal ratio of the probes, **Y,** to the target, **R,** for triplex hybridisation (2 to 1, respectively), saturation of polypyrimidine sites starts earlier for lower density of the probes. For the 100 probes/MNP and 50 probes probes/MNP, we estimated saturation of the optomagnetic signal to be upon reaching 4 nM and 2 nM concentration of polypurine target, respectively. The plots reflect these proportions.

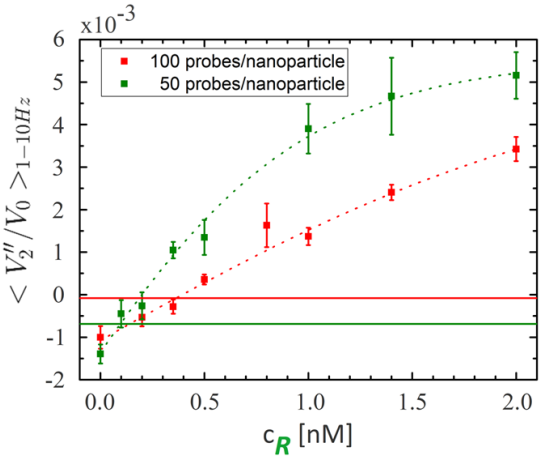

Fig. S5: Detection of triplex DNA via MNP agglutination at two different densities of p-DNA. $\langle V_2''/V_0 \rangle_{1-10\,\mathrm{Hz}}$ vs. concentration of polypurine target DNA.

References

1. A. Mezger, J. Fock, P. Antunes, F. W. Østerberg, A. Boisen, M. Nilsson, M. F. Hansen, A. Ahlford and M. Donolato, *ACS Nano*, 2015, **9**, 7374–7382.